SECURITY CLASSIFICATION OF THIS PAGE

PORT DOCUMENTATION PAGE

(2)

AD-A243 095

	1b RESTRICTIVE MARKINGS
	3 DISTRIBUTION/AVAILABILITY OF REPORT Unlimited
4 PERFORMING ORGANIZATION REPORT NUMBER(S) 11	5 MONITORING ORGANIZATION REPORT NUMBER(S)
6a NAME OF PERFORMING ORGANIZATION NIST	6b OFFICE SYMBOL (If applicable)
7a NAME OF MONITORING ORGANIZATION ONR	
6c ADDRESS (City, State, and ZIP Code) A329, Materials Building Gaithersburg, MD 20899-0001	7b ADDRESS (City, State, and ZIP Code) Code 1131 800 N. Quincy Street Arlington, VA 22217-5000
8a NAME OF FUNDING/SPONSORING ORGANIZATION ONR	8b OFFICE SYMBOL (If applicable)
9. PROCUREMENT INSTRUMENT IDENTIFICATION NUMBER N0014-90-F-0011	
8c ADDRESS (City, State, and ZIP Code)	10 SOURCE OF FUNDING NUMBERS

PROGRAM ELEMENT NO	PROJECT NO	TASK NO	WORK UNIT NO

11 TITLE (Include Security Classification)

Chemical Vapor Deposited Diamond

12 PERSONAL AUTHOR(S)
Albert Feldman, Edward N. Farabaugh and Lawrence H. Robins

13a. TYPE OF REPORT	13b. TIME COVERED	14 DATE OF REPORT (Year, Month, Day)	15 PAGE COUNT
interim	FROM _____ TO _____	91-9-27	44

16 SUPPLEMENTARY NOTATION

17 COSATI CODES			18. SUBJECT TERMS (Continue on reverse if necessary and identify by block number)
FIELD	GROUP	SUB-GROUP	This document has been approved for public release and sale: its distribution is unlimted.

19 ABSTRACT (Continue on reverse if necessary and identify by block number)

There is considerable interest in using diamond for numerous applications because of the development of methods that allow for the deposition of diamond by chemical vapor deposition (CVD) techniques over large areas. The interest in new applications for diamond rests on combinations of superior properties that diamond possesses. These extreme properties, which are based on measurements in bulk single crystal diamond, include greatest hardness, highest elastic moduli, and highest thermal conductivity at room temperature of any material. Other important properties include optical transparency over an extensive wavelength range from the ultraviolet through the far infrared, high electrical resistivity, dopability to be a semiconductor, low permeability to diffusion, chemical inertness, and low coefficient of friction.

20 DISTRIBUTION/AVAILABILITY OF ABSTRACT	21 ABSTRACT SECURITY CLASSIFICATION
☒ UNCLASSIFIED/UNLIMITED ☐ SAME AS RPT ☐ DTIC USERS	unclassified
22a NAME OF RESPONSIBLE INDIVIDUAL	22b TELEPHONE (Include Area Code) / 22c OFFICE SYMBOL

DD FORM 1473, 84 MAR — 83 APR edition may be used until exhausted. All other editions are obsolete. SECURITY CLASSIFICATION OF THIS PAGE

Enclosure (1)

OFFICE OF NAVAL RESEARCH

Contract N00014-90-F-0011

R&T Project No. IRMT 025

TECHNICAL REPORT No. 11

CHEMICAL VAPOR DEPOSITED DIAMOND

Albert Feldman, Edward N. Farabaugh and Lawrence H. Robins

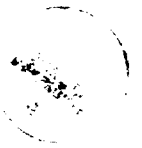

submitted to

Ceramics Films and Coatings

National Institute of Standards and Technology

Ceramics Division

Gaithersburg, MD 20899

September 27, 1991

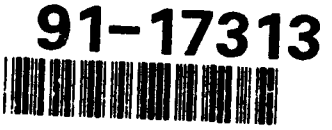

CHEMICAL VAPOR DEPOSITED DIAMOND*

ALBERT FELDMAN, EDWARD N. FARABAUGH, AND LAWRENCE H. ROBINS
Ceramics Division
Materials Science and Engineering Laboratory
National Institute of Standards and Technology
Gaithersburg, Maryland 20899

Contents

INTRODUCTION

There is considerable interest in using diamond for numerous applications because of the development of methods that allow for the deposition of diamond by chemical vapor deposition (CVD) techniques over large areas. The interest in new applications for diamond

---

rests on combinations of superior properties that diamond possesses. These extreme properties, which are based on measurements in bulk single-crystal diamond, include greatest hardness, highest elastic moduli, and highest thermal conductivity at room temperature of any material. Other important properties include optical transparency over an extensive wavelength range from the ultraviolet through the far infrared, high electrical resistivity, dopability to form a semiconductor, low permeability to diffusion, chemical inertness, and low coefficient of friction.

The principal uses of bulk diamond, either natural or man made by the high-pressure/high-temperature process, have been abrasives from diamond powders and cutting tools from polycrystalline diamond compacts, machining with diamond crystal points, heat dissipating substrates for small electronic components and laser diodes, windows for specialized applications, and diamond scalpel blades. CVD diamond is already being used in cutting tools for nonferrous materials, x-ray windows, and loud speakers. Other uses expected soon are large area, heat dissipating substrates for electronics and mask supports for x-ray lithography.

HISTORICAL BACKGROUND

Researchers have attempted to employ synthetic means to produce diamond for many years. Graphite is the stable form of carbon at room temperature and at one atmosphere (10^5 Pa) of pressure and, under these conditions, diamond is a metastable phase of carbon. Diamond exists as a stable phase only at extremely

high pressures and temperatures. Graphite can be converted directly to diamond but this process requires pressures that are extremely high (>1.2 10^{10} Pa). An explosive shock method was developed to produce diamond directly from graphite; however, the diamond is produced as small particles ranging in size from submicrometer to several micrometers. The first commercially successful method to synthesize diamond was a high-pressure/high-temperature process developed at the General Electric Company (1). In this process diamond is produced by precipitation from a solution of graphite and a metal catalyst such as iron, nickel, or cobalt. The process is conducted at pressures above 4.5 GPa and temperatures greater than 1100 °C. This process is generally used to produce polycrystalline diamond from graphite. By employing temperature gradients and charges of polycrystalline diamond in the high-pressure/high-temperature apparatus, it is possible to produce gem quality diamonds. However, the maximum dimension of these diamonds has been limited to less than 2 cm. Most recently, a diamond crystal of isotopically pure ^{12}C has been produced which shows excellent optical quality and which has a thermal conductivity that exceeds the thermal conductivity of type IIa diamond by 50% (2). Prior to this work, natural type IIa diamond was considered the diamond of highest purity with a room temperature thermal conductivity of about 21 W/cm/K, the highest of any material.

Methods for depositing diamond from the gas phase have been under investigation for many years. At about the time that General Electric developed its high-pressure/high-temperature process, Eversole at Union Carbide was able to produce diamond particles from carbon monoxide gas (3). At about the same time,

work on depositing diamond from the gas phase began in the Soviet Union under Deryagin (4). These early gas phase processes had two principal problems, graphitic material deposited simultaneously with the diamond, and the growth rate of diamond was very low. A key discovery was made at Case Western Reserve (5) that eventually led to high rate growth methods. In a study of diamond growth from a feed gas containing methane, it was found that atomic hydrogen etched the graphitic impurities while leaving behind the diamond. The Deryagin group made use of this information to grow diamond at practical growth rates by using large quantities of hydrogen in its gas mixtures (6). Diamond deposition depended on employing an energetic process for converting molecular hydrogen to atomic hydrogen, which is now recognized as essential for diamond growth from the gas phase in most CVD processes that employ hydrocarbon gases. Recently, a group at Rice University has found that halogenated gases can also be used to produce diamond by a CVD method that did not require an energetic activation process (7).

The first widely used methods for depositing diamond were developed at the National Institute for Research in Inorganic Materials (NIRIM) in Japan. These included the hot filament CVD method (8) and the microwave plasma CVD method (9). Both of these methods employed feed gas mixtures of methane in hydrogen. The deposition rates are low by today's standards, although many researchers are using these methods in order to understand the deposition process. More recently, hot plasma (10) and oxy-acetylene torch (11) methods have been developed that exhibit very high growth rates and material of high quality. All of the above methods produce polycrystalline diamond.

Recent publications report that single-crystal diamond can also be grown by ion implantation of carbon into a copper surface followed by an annealing process (12).

METHODS OF DEPOSITION

The earliest method to produce diamond at reasonable deposition rates was developed in the Soviet Union (13). Figure 1 is a schematic diagram of the experimental apparatus. The method is based on transport of carbon from a graphite susceptor to the substrate by means of the hydrogen catalysis. The

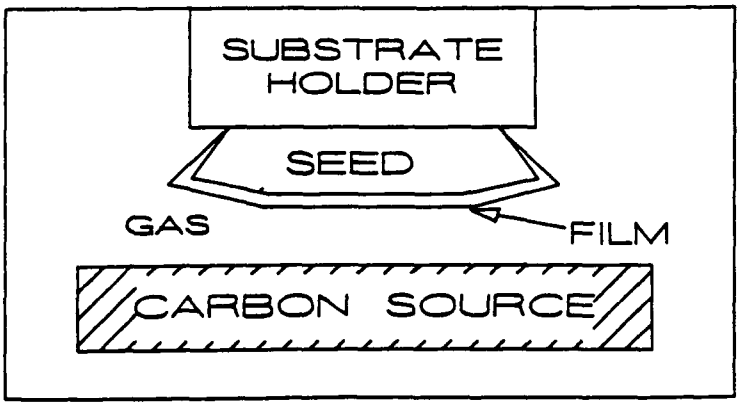

Figure 1. Schematic diagram of diamond deposition as described by Spitsyn (13). The gas consists of hydrogen, atomic hydrogen, methane, acetylene, and other hyrocarbons.

graphite was heated by optical means to a temperature of about 2000 °C. A fraction of the hydrogen gas in contact with the graphite was converted to atomic

hydrogen, which etched the graphite, resulting in a number of hydrocarbon gas species such as methane and acetylene. The hydrocarbons diffused to the cooler substrate, held at about 1000 °C, where it reacted to deposit diamond.

The hot filament method was the first practical method to produce diamond in a systematic way because of a greater degree of process control (8). Figure 2 shows a schematic diagram of a hot filament reactor at NIST. A hydrogen and methane feed gas mixture is allowed to pass over a hot filament. Typical deposition conditions are: substrate temperature, 600 to 950 °C, filament temperature, 1800 to 2100 °C; gas pressure, (2.5 to 13) × 10^3 Pa (20 to 100 torr); flow rate, 40 to 100 cm^3/min; and, methane fraction in the feed gas, 0.1 to 5%. The quality of the diamond produced, as revealed by Raman spectroscopy, improves with decreasing methane fraction in the feed gas.

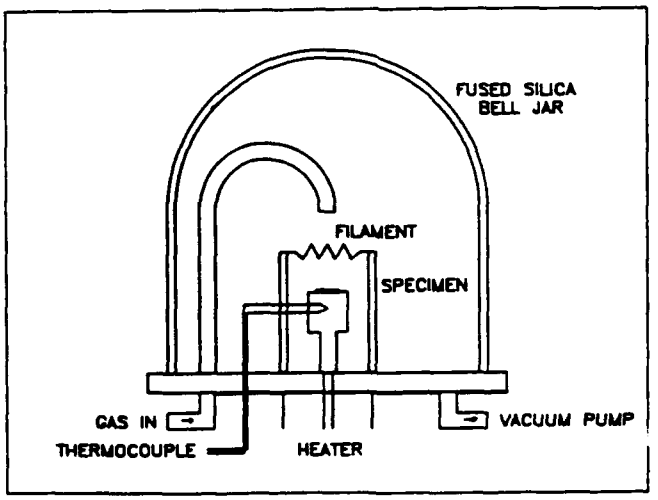

Figure 2. Schematic diagram of hot filament CVD reactor for depositing diamond.

The microwave plasma CVD method was the next practical method to be developed (9). Figure 3 shows

a schematic diagram of a microwave system. A heated substrate is placed below a plasma ball sustained by a

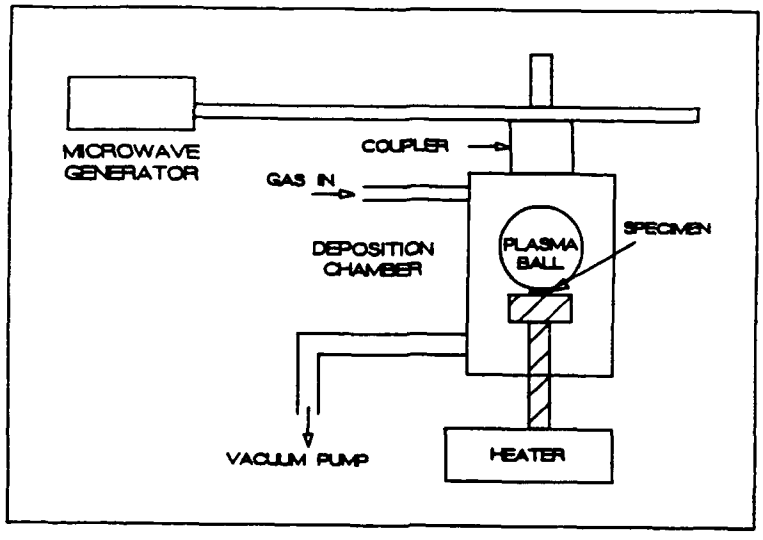

Figure 3. Schematic diagram of microwave plasma CVD reactor for depositing diamond.

microwave discharge. The substrate can be heated by the plasma alone or with a separate heating source. The deposition parameters are similar to those in the hot filament reactor. Adding oxygen to the feed gas mixture improves the quality of the diamond (14). Most commercial microwave systems operate at a frequency of 2.45 GHz.

Modulation of the gas composition with time in the microwave reactor acts to increase the growth rate and to improve the diamond quality (15). For example, a gas mixture of 5% methane and 95% hydrogen flowed in the chamber for four minutes, followed by a gas mixture of 1% oxygen and 99% hydrogen in the chamber for two minutes would represent one period of a cyclical process. The process periodically acts to deposit diamond and then etch away any nondiamond

impurities that may deposit with the diamond.

The hot filament and microwave plasma methods are low deposition rate methods with deposition rates ranging from 0.1 to 1 μm/hr for reasonably high quality diamond. Other deposition methods have been developed that result in much higher deposition rates. All of these methods rely on the use of thermal plasmas at high temperatures or combustion processes. These include DC plasma deposition (16), radio frequency (RF) plasma deposition (17), and the oxy-acetylene torch (11). The high deposition rates in these systems are attributed to the large amount of atomic hydrogen generated at the high plasma temperatures. However, because of the large amounts of heat generated by these techniques, extensive use of water cooling is required.

Growth rates as high as 930 μm/hr have been reported for the DC plasma torch method (18). These systems contain a nozzle equipped with several gas inlets that allow for various mixtures of Ar, H_2, hydrocarbons, and oxygen-containing organic compounds. Deposition is usually conducted in a chamber below atmospheric pressure. DC plasma deposition is used for some of the commercially produced CVD diamond. One problem with this type of system is electrode erosion which can lead to contamination of the deposited diamond.

Deposition rates of about 200 μm/hr have been achieved with an RF plasma torch. The RF generator typically operates at a frequency of 4 MHz with a power output up to 50 kW. Gas mixtures of Ar, H_2 and methane are utilized at flow rates of tens of liters per minute. Problems with this technique include

plasma instabilities, power transfer inefficiencies, and nonuniform depositions.

The oxy-acetylene torch method is receiving considerable attention as a means for depositing high quality diamond at high deposition rates. Diamond has been found to deposit in the reducing region of an oxygen-poor flame. The greater the amount of oxygen in the flame, the higher the quality of the diamond; however, the growth rate decreases with increasing oxygen content in the flame. An advantage of this method is that diamond can be grown in the open atmosphere. Recent reports indicate this method can be used to significantly increase the size of diamond seed crystals at rapid growth rates. This is accomplished at substrate temperatures as high as 1600 °C, which is considerably higher than the highest temperature normally expected for diamond growth (1000 °C). It is believed that growth occurs at these high temperatures because the abundance of atomic hydrogen in the flame prevents the graphitization of the material.

Halogenated compounds have been used to grow diamond by a direct CVD process without the need for a activating process or for atomic hydrogen. Furthermore, deposition of diamond has been observed at temperatures as low as 300 °C (7). Mixtures of hydrogen and fluorine containing gases such as CF_4 flow through a monel tube containing a thermal gradient. The highest temperature at the center of the tube is ~950 °C, decreasing to 250 °C near the tube ends. One problem that must be addressed with this method is the removal of gases, such as HF, that are toxic and corrosive. The quality of the diamond produced by this method is yet to be evaluated.

Electronic applications will require large area, single crystal diamond coatings; this is one of the major goals of CVD diamond research. Recently, thin single-crystal diamond has been deposited onto a copper substrate (12). Carbon ions were initially implanted into the surface of a single-crystal copper substrate. Carbon has negligible solubility in copper. Upon heating with a pulsed high-power laser beam, the copper at the surface melts. Due to the high thermal conductivity of copper, the heat rapidly dissipates into the bulk of the copper crystal causing rapid solidification. The solid-liquid interface moves rapidly toward the crystal surface expelling the implanted carbon. Due to the rapid cooling, the carbon has insufficient time to crystallize into the stable phase, which is graphite, but does crystallize into the diamond phase. This latter process is not a CVD process; however, the CVD process can be used to greatly increase the thickness of the single-crystal diamond film, once a large area single-crystal surface has been created.

GROWTH AND QUALITY OF CVD DIAMOND

Angus and Hayman (19) have discussed the fundamental processes leading to nucleation and growth of diamond. In practice, the substrate upon which the diamond is grown is usually rubbed, scratched or polished with diamond powder. It is not yet clear how this process promotes nucleation. It may be due to exposure of chemically active nucleation sites on the surface of the substrate, or it may be due to residual diamond remaining on the substrate as seeds for

diamond growth. Diamond appears to grow best on carbide forming substrates such as silicon or molybdenum. Diamond can also be grown on other substrates such as silicon carbide, silicon nitride, mullite, fused silica or sapphire. Most researchers use silicon as the substrate material. Silicon has the advantages of being readily available and of having a linear thermal expansion that is close to that of diamond from room temperature to 950 °C. Large differences in the thermal expansion over this temperature range usually lead to fracture of the diamond or the substrate or to delamination of the diamond from the substrate. Figure 4 compares the linear thermal expansion of diamond with several substrate materials. Silicon nitride has a good

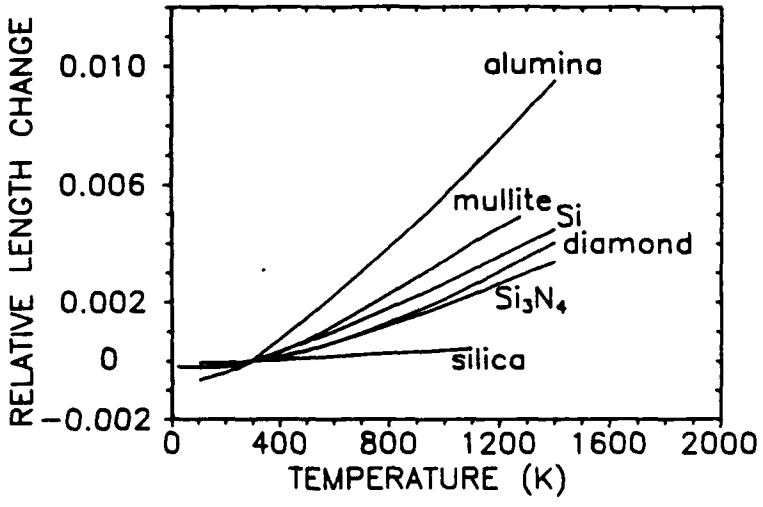

Figure 4. Linear thermal expansion of diamond and several other materials.

thermal expansion match and for this reason is being used as a substrate material for diamond coated cutting tools.

Diamond nucleates as discrete particles on the

surface of the substrate. When the diamond particle size approaches the interparticle separation distance, the particles merge to form a continuous layer. Thus, the surface of a diamond film is rough. The

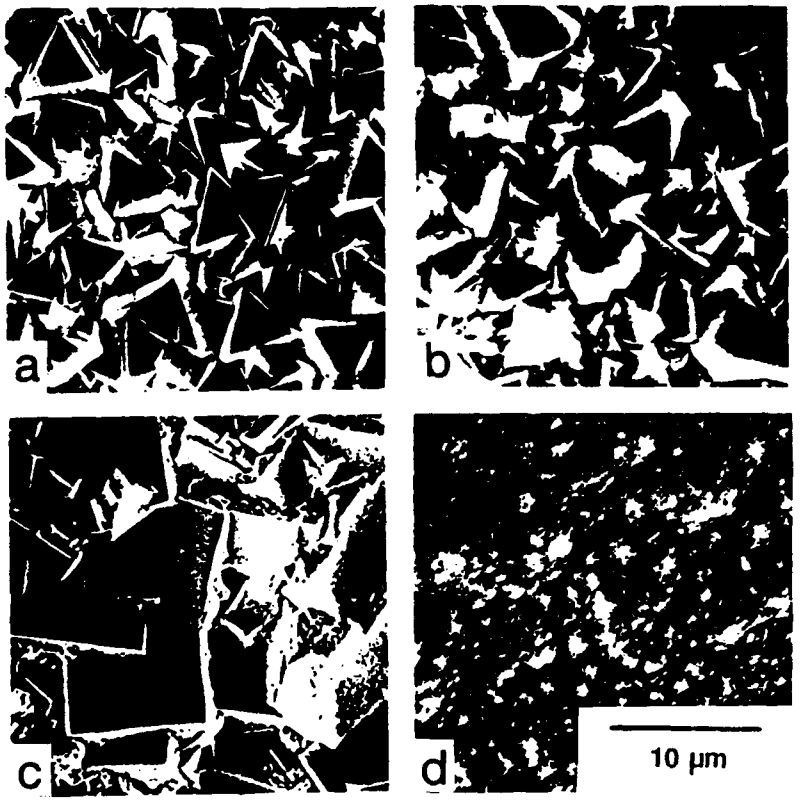

Figure 5. Morphologies of films grown in a hot filament CVD reactor: a) triangular {111} morphology; b) {110} morphology; c) {100} morphology; d) "cauliflower" morphology.

morphology of the film depends upon growth conditions. The film also shows a preferential orientation. Let us consider diamond produced in a hot filament or a microwave reactor using methane and hydrogen as the feed gas. At the lowest methane concentrations, the films produced show a triangular morphology where the triangular faces are {111} planes. The films show preferential orientation of the <111> direction normal

to the film surface. At higher methane concentrations, a pyramidal morphology is observed which is indicative of preferential orientation of <110> directions normal to the film surface. At even higher methane concentrations, the films show predominantly square faceting, corresponding to {100} planes, and the <100> directions are preferentially oriented normal to the film surface. At even higher methane concentrations, the surfaces have a cauliflower appearance and faceting is not observed. Figure 5 shows examples of the different morphologies observed in a scanning electron microscope.

Several techniques are used to evaluate the diamond produced. The simplest is x-ray diffraction which is used to verify the presence of the crystalline diamond phase. Figure 6 compares an x-ray pattern of natural diamond powder with an x-ray pattern of a diamond film produced at NIST. A modified Debye-Scherrer wide film technique was used to obtain these patterns. The discrete spots seen in the diamond film pattern are due to diffraction from the single-crystal silicon substrate. A disadvantage of this type of x-ray diffraction is its insensitivity to the presence of amorphous carbon phases that are usually present as impurities in the diamond.

Auger spectroscopy is another technique that has been used to examine diamond. Distinct Auger spectra are observed from graphite, diamond, and amorphous carbon (20,21). However, since this technique is sensitive only to the first few atomic layers on the surface of the specimen, care must be taken to avoid erroneous identifications when confirming for the presence of diamond.

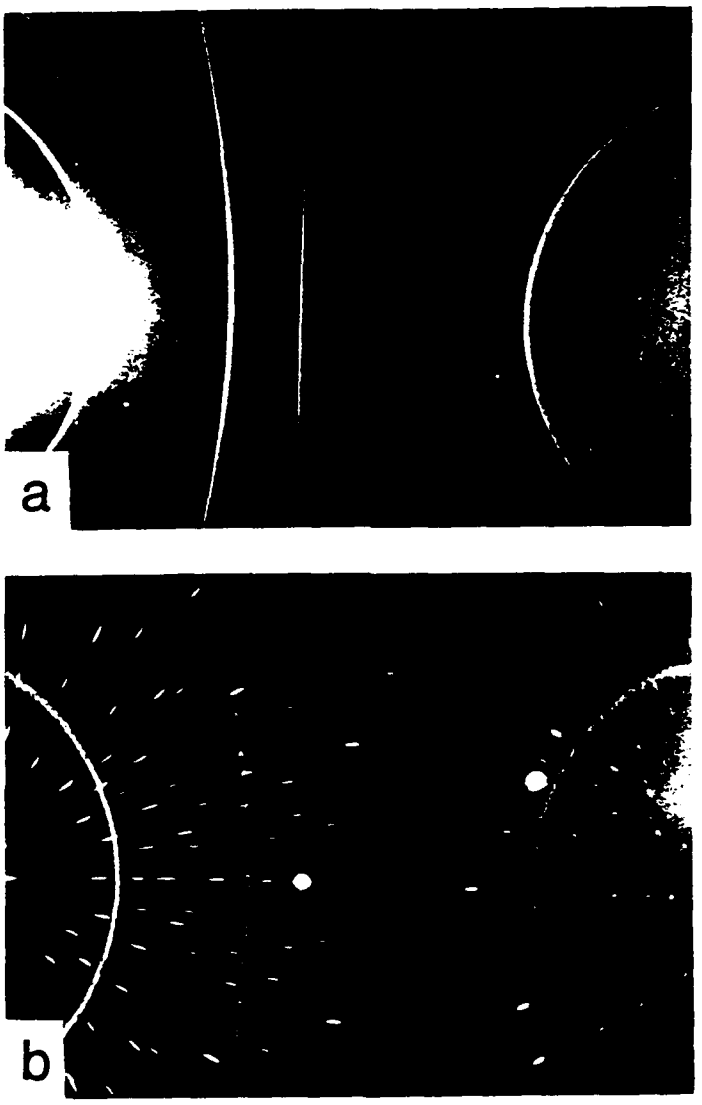

Figure 6. X-ray diffraction patterns of: a) natural diamond powder and b) of CVD diamond produced at NIST.

Diamond films may also be characterized by electron energy loss spectroscopy (EELS) (21). As with Auger spectroscopy, diamond and graphite possess distinct EELS spectra. Recently, EELS has been useful in determining the relative amounts of diamond

chemical bonding (sp^3) and graphitic bonding (sp^2) in diamondlike hydrogenated carbon films (22).

Raman spectroscopy has been accepted as the method of choice for evaluating the quality of the diamond produced. The Raman spectrum of diamond consists of a single sharp peak located at 1332 cm^{-1} wavenumber shift relative to the exciting laser source (23). This line comes from scattering of a photon

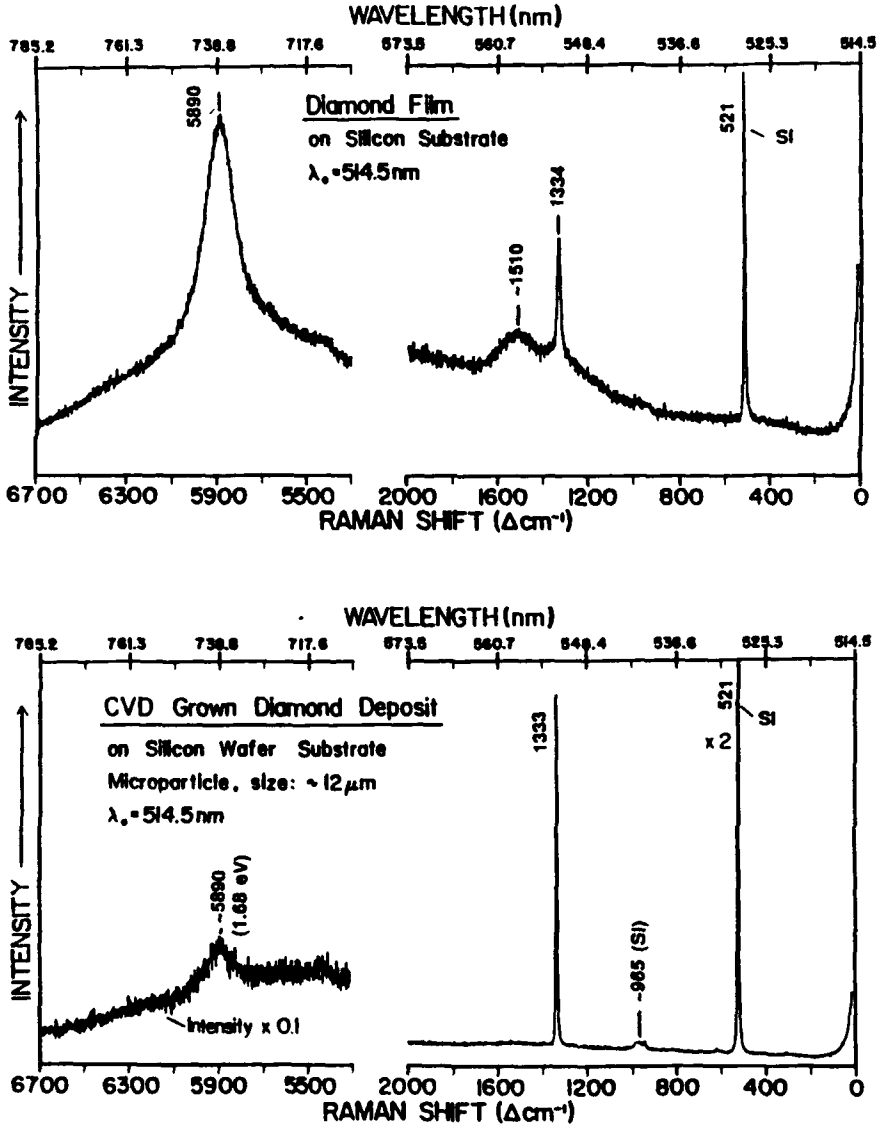

Figure 7. Raman spectra of a CVD diamond film and a CVD diamond particle.

from the transverse optical phonon of diamond. However, when one examines the Raman spectrum of CVD diamond, one usually observes a more complicated spectrum composed of several spectral features. Figure 7 shows a typical Raman spectrum of CVD diamond excited by the 514.5 nm line of an argon-ion laser. In addition to the sharp line at 1334 cm^{-1}, (small deviations in the diamond line position are believed to be due to internal stress) there is a broad peak centered near 1500 cm^{-1} that is attributed to graphitic or sp^2 bonding, a broad luminescence background of undetermined origin, and a luminescence band at 5890 cm^{-1} associated with point defects in the material. It is found that the intensity of the graphitic band correlates positively with the intensity of the background luminescence, and to a lesser extent, with the width of the diamond Raman peak (24). Figure 7 also shows the Raman spectrum of a CVD diamond particle. The spectrum is dominated by the diamond Raman peak. Raman spectra from diamond particles usually show much less fluorescence background and smaller graphitic carbon peaks than diamond films suggesting that these spectral features are associated with the grain boundaries in the polycrystalline films. The luminescence feature seen at 5890 cm^{-1} is believed to be due to silicon incorporated in the diamond lattice (25).

An interesting means of examining diamond on a microscopic scale is cathodoluminescence imaging and spectroscopy. In this method, the specimen is placed in a scanning electron microscope and the optical radiation emitted by the specimen is collected by a photodetector. The optical signal arises when valence band electrons are excited above the fundamental energy gap of the diamond into the conduction band by

the energetic electron beam (>10 kV) in the SEM. The electrons in the conduction band can decay to defect states within the band gap. The electrons can lose energy from these defect states by emitting optical radiation whose spectral features are characteristic of the defect center.

The cathodoluminescence provides an optical image of the specimen as the electron beam scans over the specimen. This image can be compared to the secondary electron image customary observed with the electron microscope. Figure 8 shows a

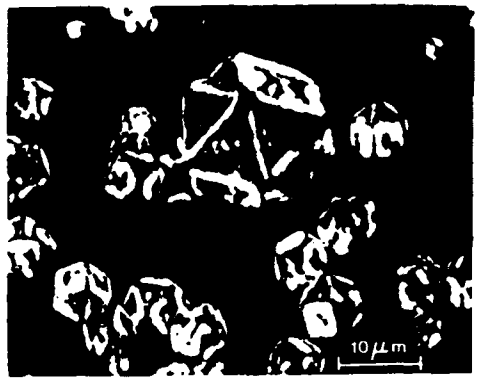

CL IMAGE

SECONDARY-ELECTRON IMAGE

Figure 8. Cathodoluminescence image of diamond particles and the corresponding SEM image.

cathodoluminescence image and an SEM image of diamond particles deposited by CVD. The image provides information regarding the distribution of luminescent defects in the diamond. However, the interpretation of the image in terms of defect densities is not necessarily straightforward because the intensity of the luminescence from a particular defect species depends not only on the number density of that species but also on the densities of other species that give rise to competing decay processes.

By a spectral analysis of the cathodoluminescence spectrum, one can deduce the nature of the defect centers. This identification is based on a large body of work in which the luminescence spectra of many defects have been identified. Figure 9 is the cathodoluminescence spectrum of a diamond film that shows several spectral features often observed in CVD diamond. These features have been associated with particular defects: a sharp line at 1.68 eV believed to be due to a silicon impurity introduced during deposition (this

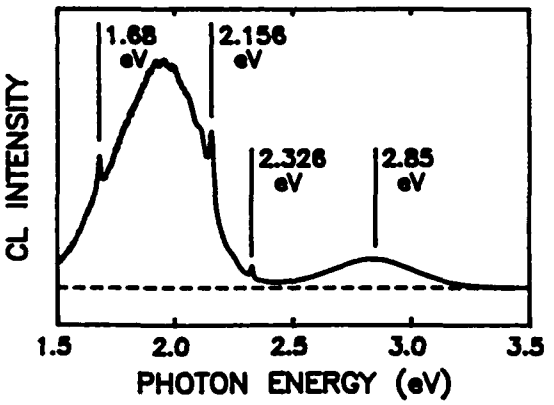

Figure 9. Cathodoluminescence spectrum of CVD diamond film showing principal spectral features.

feature is identical to the luminescence line observed at 5890 cm^{-1} in the Raman experiment); a line at 2.156 eV, with an associated vibronic band centered near 2 eV, due to a nitrogen-vacancy (N-V) complex; a line at 2.326 eV due to a different N-V complex; and, a broad violet band centered at 2.85 eV, due to a dislocation related defect. A line at 3.188 eV due to a nitrogen interstitial-carbon complex has also been observed in some CVD diamond films.

THERMAL PROPERTIES OF CVD DIAMOND

High thermal conductivity makes diamond very desirable for heat dissipation applications. However, even in bulk diamond, the thermal conductivity can vary considerably, depending on the presence of defects and impurities. The question arises whether the thermal conductivity of CVD diamond can be as high as the that of the best bulk diamond. Furthermore, the measurement of thermal conductivity in specimens with high values is difficult, especially when the specimens are in thin film form.

Ono et al. (26) have systematically measured the thermal conductivities of a series of diamond film specimens prepared in a microwave reactor. They measured the thermal conductivity as a function of the methane/hydrogen ratio used in the specimen preparation which varied from 0.1% to 3%. The specimens, which consisted of bare diamond strips coated with black paint, were supported in vacuum between two heated posts. Radiative cooling resulted in a temperature profile that varied approximately

parabolically with distance from the posts. The temperature profile was measured with a thermograph. By considering the radiative cooling and the heat flow in the strips, the authors calculated the thermal conductivities of the films. The specimen prepared with 0.1% methane/hydrogen ratio showed the highest thermal conductivity, 10 W/cm/K. This is about one half that value of type IIa diamond but is still respectably high. The thermal conductivity decreased rapidly with increasing methane/hydrogen ratios and this was found to correlate well with an increasing sp^2 component in the Raman spectrum.

Morelli et al. (27) used a steady state four probe technique to measure the thermal conductivity of two freestanding films of CVD diamond as a function of temperature between 10 K and 300 K. The low temperature values were as much as two orders of magnitude lower than the values for type IIa diamond; however, the values significantly increased with increasing temperature so that at 300 K the values were comparable to the highest values obtained by Ono et al. The small values of thermal conductivity at low temperatures were attributed to phonon scattering from grain boundaries.

Albin et al. (28) measured the thermal diffusivity of two CVD diamond films. Thermal diffusivity, α, is related to thermal conductivity, κ, by $\alpha=\kappa/(\rho C)$, where ρ is the density and C is the specific heat. The authors focussed a repetitively pulsed Nd:YAG laser onto a specimen consisting of CVD diamond on a silicon substrate. The time dependence of the temperature distribution across the specimen along a line that passed through the heated spot was measured with an infrared camera as a set of

successive images. The effective thermal diffusivity of the specimen was calculated from the computed phase and amplitude of the temperature profile away from the heated spot. If one assumes that the substrate thickness, d_s, and film thickness, d_f, were much less than the thermal diffusion lengths in both materials at the modulation frequency used, the effective thermal diffusivity, α_e, is given by

$$\text{Eq. (1)} \qquad \alpha_e = \frac{\alpha_f \alpha_s (\kappa_f d_f + \kappa_s d_s)}{\alpha_s \kappa_f d_f + \alpha_f \kappa_s d_s}$$

Using this equation, the authors computed α_f to be about 8 cm^2/s for two CVD diamond films 16 μm and 32 μm thick. The corresponding thermal conductivity is 14 W/cm/K if the bulk values ρ=3.5 g/cm^3 and C=0.51 J/g/K are assumed to hold for CVD diamond. This is the largest value of thermal conductivity reported for CVD diamond. This method measures the component of the thermal diffusivity parallel to the surface.

Feldman et al. (29) have used photothermal radiometry to measure the thermal diffusivity of a CVD diamond plate 0.24 mm thick. The method is similar to that of Albin et al. A modulated laser beam from an argon-ion laser is focused onto the surface of the diamond plate which has a black carbon coating for increasing the surface absorptance at the laser wavelength and the surface emittance in the infrared. The infrared radiation emitted by the heated surface is detected with an indium-antimonide detector. The phase of the thermal signal as a function of

modulation frequency will depend on the thermal diffusivity of the specimen. The thermal conductivity obtained assuming bulk values for ρ and C was 5.5 W/cm/K.

Most recently Lu and Swann (30) have used the method of Cielo (31) to measure the thermal diffusivity of CVD diamond. The method is similar to that of Albin et al. except that the beam of a ruby laser is focused to a ring of light on the diamond plate with an axicon lens. The radius of the ring was 11 mm, thus the method is applicable to large area specimens. A mercury-cadmium-telluride detector placed behind the specimen was used to detect the thermal radiation emitted by the back surface of the specimen at the center of the ring. For a thin specimen, the temperature at the center of the heated ring is given by

$$\text{Eq. (2)} \qquad T=E/(4\pi\rho\alpha t)\exp[-r^2/(4\alpha t)]$$

where E is the absorbed energy per unit thickness, r is the focused ring radius, and t is the time after the laser pulse. The maximum temperature at the center of the ring occurs at a time, $t=r^2/(4\alpha)$, after the laser pulse. For a CVD diamond plate several hundred micrometers thick, the authors obtained a transverse thermal conductivity of 12 W/cm/K. The authors checked the accuracy of their measurements by performing the measurements on specimens of copper, silver, aluminum, and aluminum nitride. Agreement with published values was better than 8%.

The recent discovery of high thermal conductivity in isotopically pure ^{12}C diamond was based on photothermal deflection measurements (2). During the measurement the surface of the specimen is heated with a modulated laser beam in a manner similar to that in the photothermal radiometry method mentioned above. A second, low power probe laser beam is made to skim the surface of the specimen in the vicinity of the heated spot. Due to transfer of heat from the specimen surface to the air above the specimen, a modulated thermal gradient will be present in the air that acts to periodically deflect the probe beam. The deflection is measured as a function of the distance of the probe beam from the heating beam. An analysis of the phase and amplitude of the probe beam deflection allows for calculating the thermal diffusivity of the specimen. Because the diamond specimen was very transparent, it was necessary to coat the surface of the specimen with an absorbing layer in order to perform the measurements. A value of 34 W/cm/K was obtained for the thermal conductivity of the isotopically pure diamond.

OPTICAL PROPERTIES

Pure diamond has the widest transmission range of any solid material. It is transparent from the electronic absorption edge at 225 nm through the far infrared except for a region of absorption between 3 and 6 μm. Most crystalline materials absorb infrared radiation in particular wavelength regions due to the excitation of lattice vibrations (or phonons) by the infrared radiation. Because of the symmetry of the

diamond lattice, no absorption should occur due to excitation of single phonons. Absorption does occur due to excitation of two or more phonons, but this absorption is relatively weak. This is the process responsible for the region of absorption between 3 and 6 μm observed in all diamond crystals. Lattice defects can disrupt the perfection of the diamond lattice, leading to infrared absorption due to single phonon excitations. This absorption process is very weak and great care must be exercised for its observation in thin specimens. In applications requiring thick optical components, these weak absorption processes can produce large absorptances that can be deleterious. Absorption can also occur due to the presence of impurities in the diamond. Both nitrogen and boron, impurities occurring naturally in diamond, increase the wavelength range of absorption in natural diamond. The classification of diamond into types I and II is based on absorption due to nitrogen impurities. Type II diamonds do not display the characteristic ultraviolet and infrared absorption bands associated with nitrogen impurities.

Optical transmission measurements have been made on CVD diamond films principally in the infrared part of the spectrum (32-39). The infrared region was examined because the growth surface of CVD diamond is usually too rough to transmit light at visible wavelengths without excessive optical scatter. Typical average roughnesses, R_a, are 0.1 to 0.5 μm. Several authors have published transmission data showing typical spectral features: a decrease in the transmittance with increasing wavenumber above 1000 cm^{-1}, an absorption band due to C-H stretching near 2800 cm^{-1}, and an oscillatory transmittance due to beam interference in the specimen. The two photon

absorption region usually coincided with the region of optical scatter and, due to the small thicknesses of the specimens, was not strongly evident. However, transmittance measurements in thicker specimens have shown significant absorption effects. Gatesman et al. (39) were able to measure absorption that was attributed to free carriers in a film 76.2 μm thick. Figure 10 shows their fit to optical transmission data obtained in a Fourier transform infrared spectrometer. The fit includes models for free carrier absorption and surface roughness.

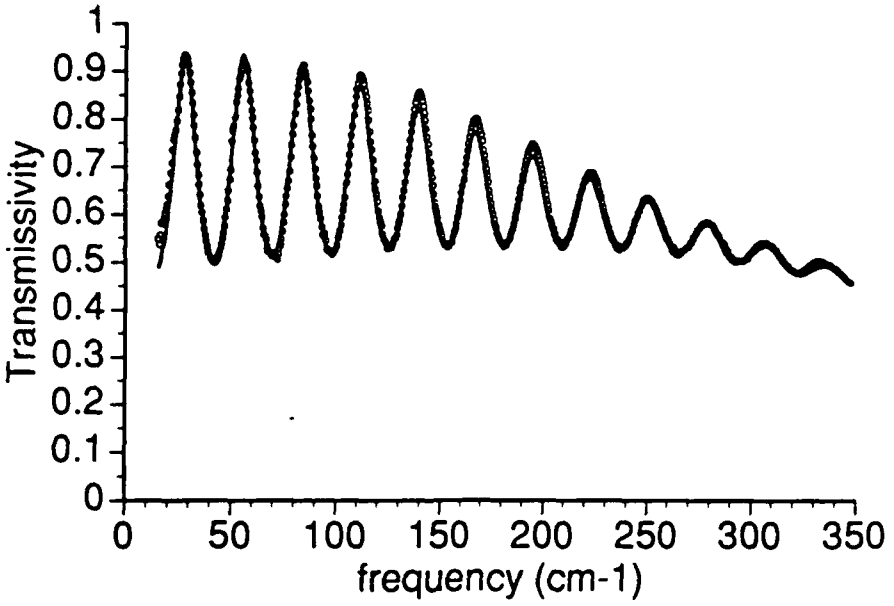

Figure 10. Transmission spectrum of CVD diamond measured by Gatesman et al. (39). (Reprinted with permission of the author.)

An important region of the spectrum for optical applications of CVD diamond is between 8 and 12 μm. As mentioned above, diamond should be transparent over this wavelength range. Until recently, CVD diamond had not been available with sufficient quality and thickness to observe the limits of optical absorption

between 1250 and 833 cm^{-1} due to weak single phonon processes. In a recent study, Klein et al. (40) have reported on infrared transmission measurements performed on good quality diamond films 0.2 to 0.4 mm thick grown by microwave plasma and hot filament CVD methods. Spectra taken in a Fourier transform spectrometer over the wavenumber range 500 to 4000 cm^{-1} show three distinct absorption regions associated with one phonon, two phonon, and three phonon absorption. A small absorption is found in the region where one phonon absorption should occur suggesting that symmetry-breaking defects are indeed present. By comparing the peaks in the absorptance spectra with expected critical points in the phonon spectrum determined by neutron diffraction (41), Klein et al. were able to attribute spectral features in the absorptance spectrum to particular phonons.

By careful preparation of the substrate prior to diamond deposition, it is possible to produce reasonably smooth diamond films that are transparent in the visible and near ultraviolet region of the spectrum. The substrate, typically silicon, is rubbed for approximately one minute against a one micrometer diamond powder placed on a glass plate. This process causes a high density of diamond nucleation sites on the substrate; thus, the diamond particles that nucleate on the substrate merge to form a continuous film at thicknesses significantly less than one micrometer. The resultant films show root-mean-squared surface roughnesses ~0.02 μm as long as the film thickness is not much greater than 1 μm. Transmittance measurements are conducted on unsupported diamond film specimens in which the substrate material is etched away; reflectance measurements are also be made. Figure 11 shows the

transmittance spectrum of one such diamond film 0.8 μm thick (42). The film is transparent to photons with energies less than the absorption edge at 5.45 eV (225 nm). The oscillations in the spectrum are due to interference effects. By fitting transmittance and reflectance data to appropriate models, one can obtain surface roughness, refractive index, thickness, and absorption coefficients of the films.

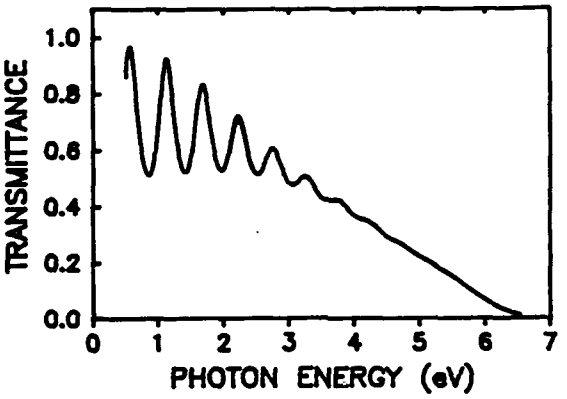

FIGURE 11. Transmission spectrum of an optically transparent diamond film.

Refractive index is an important optical property of a material. Diamond has a refractive index that is high for an ultraviolet transmitting material. The refractive index of bulk diamond has been determined in the ultraviolet, the visible and in the infrared. Table 1 lists some values at selected wavelengths (43-45). These values have been partially verified for CVD diamond.

Table 1

Refractive Index of Diamond, n, vs Wavelength (43-45)

Wavelength μm	n	Wavelength μm	n	Wavelength μm	n
0.250	2.6333	0.700	2.4062	7.00	2.3761
0.300	2.5407	2.50	2.3786	10.00	2.3756
0.400	2.4641	3.00	2.3782	15.00	2.3752
0.500	2.4324	4.00	2.3773	20.00	2.3750
0.600	2.4159	5.00	2.3767	25.00	2.3749

MECHANICAL PROPERTIES

Large area bearing-surfaces of diamond are now possible because of the CVD process. Hardness and low friction coefficient (<0.1) make diamond very desirable for this application. We must qualify the last statement because the coefficient of friction of crystalline diamond is large (0.9) in a vacuum environment when an adsorbed layer of hydrogen is absent (46). In addition, the wear and coefficient of friction depend on crystallographic orientations of the diamond surface and the sliding direction (47). Isotropic wear would be one advantage of a randomly oriented CVD diamond surface.

Jahanmir et al. (48) have compared the friction and wear characteristics of a silicon carbide ball rubbed against a bare SiC plate and rubbed against a

SiC plate coated with CVD diamond. The diamond films were deposited in a hot filament reactor in thicknesses of 2.6 and 4.3 μm. Diamond grain sizes varied from 0.5 to 2.5 μm. The experiments were conducted in a ball-on-three flat arrangement with a ball rotation rate of 100 rev/min (sliding speed of 0.038 m/s) at room temperature in air without lubrication. During a test, the normal force exerted by the ball against the flats was increased in 4 N increments; the force at each increment was kept constant for 10 min. Figure 12 shows the friction coefficient of SiC against SiC and of SiC against CVD diamond as a function of contact load. After the initial load, the coefficient of friction of the diamond coated specimen against SiC was 0.08±0.02 which is one order of magnitude less than the coefficient of friction of SiC on SiC. The wear rate on the diamond coated specimen was four orders of magnitude lower than the wear rate on the uncoated specimen.

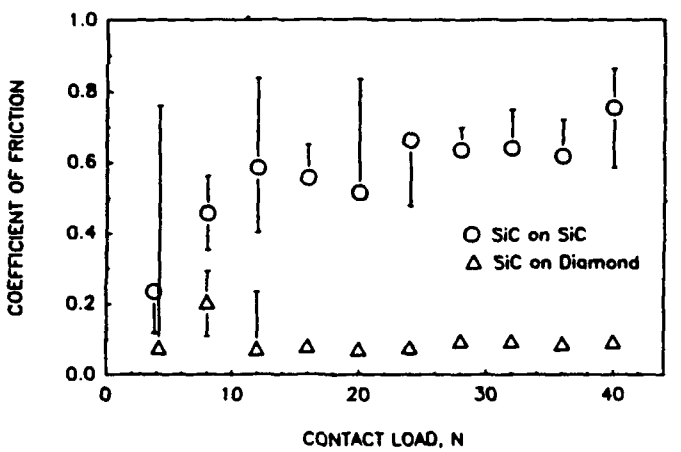

Figure 12. Friction coefficient as a function of contact load for SiC aginst SiC and SiC against diamond ball-on-flat tests.

Gardos and Ravi (49) have conducted controlled-environment tests of friction and wear on CVD diamond films. Pin-on-flat tests were conducted at low pressure (1.33×10^{-3} Pa or 10^{-5} torr) and at high pressure (13.3 Pa or 0.1 torr) over a range of temperatures from room temperature to 800 °C. Pins of SiC and SiC coated with diamond were rubbed against flat silicon substrates coated with CVD diamond by the DC plasma method. The authors found that oxygen or water adsorbates on the films lead to high friction coefficients (0.5 to 0.8) while hydrogen adsorbates lead to low friction coefficients (0.1). Experiments conducted at high temperatures at low pressure lead to increased friction coefficients due to loss of hydrogen from the film surface.

Bulge tests to determine the biaxial modulus and the residual stresses have been made on CVD diamond films (50). The biaxial modulus is related to Young's modulus, E, and Poisson's ratio, ν, by the relationship, $E/(1-\nu)$; this coefficient is the ratio of planar stress to planar strain in an isotropic medium. The test specimen was a diamond film prepared by microwave plasma CVD at a gas pressure 4000 Pa (30 torr). The feed gas ratios H_2:O_2:CH_4 by flow rate were 0.965:0.03:0.005 with a total flow rate of 500.5 cm^3/min. The film thickness was 9.61 μm. The film, which was polycrystalline, showed some (220) texture. The amount of hydrogen in the film was estimated to be 0.95%. The biaxial modulus was 960 GPa with a standard deviation of 4.3%. Depending on the value chosen for the Poisson ratio of polycrystalline CVD diamond, the authors found Young's modulus to be 864 GPa (ν=0.1) or 893 GPa (ν=0.07). These are reasonably close to the values of Young's modulus for crystalline diamond which are 1,053 GPa for <100> uniaxial stress

and 1207 GPa for <111> uniaxial stress, calculated from the elastic constant values of McSkimin et al. (51).

POLISHING CVD DIAMOND

CVD diamond films usually grow with rough surfaces that would be undesirable for many applications. Smooth diamond films can be made if the nucleation density during growth is high; however, the thickness of such films is limited to one micrometer or less, as the roughness increases with increasing film thickness.

Methods of polishing diamond films are being developed to produce smooth films. Because CVD diamond is polycrystalline and hard, it is very difficult to polish; polishing by means conventionally used to polish diamond is a very slow process. Wang et al. (37) have polished CVD diamond films on a cast iron scaife heated to 350 °C. Six weeks of polishing were required to obtain a mirror-like surface. To increase the polishing rate a sample was annealed in an atmosphere of 0.01% oxygen in argon at 1000 °C for 4 hours; the film surface turned black. In this case, the time for polishing was reduced to one week. Polishing with potassium nitrate also increased the polishing rate; however, the specimen had to be carefully monitored to avoid destruction. Polishing decreased the peak-to-valley surface roughness from 1.2 μm to less than 0.1 μm.

Yoshikawa (52) has pioneered a thermochemical

method for polishing diamond at high rates. In his method, a rotating polishing plate of iron or nickel is held at an elevated temperature inside an environmental chamber capable of supporting a vacuum. The CVD diamond surface is polished by holding it in contact with the rotating plate. In an atmosphere of hydrogen, iron produced the highest polishing rate and nickel produced nearly as high a polishing rate. No polishing action was observed with molybdenum or with cast iron plates and no polishing was observed at 700 °C or lower. At 750 °C and above, the polishing rate increased with increasing temperature. At 950 °C, the entire surface was polished after 20 min. The polishing rate also increased with applied pressure; however, excessively high pressures made the polishing process unstable. Increasing the lapping speed also increased the polishing rate. The average roughness, R_a, obtained on a 7 mm square specimen was 2.7 nm.

Frequently, the diamond surface is too rough for polishing directly. Yoshikawa has planed the surface of the specimen prior to polishing by irradiating the specimen with a Q-switched Nd-doped yttrium aluminum garnet (Nd:YAG) laser in one atmosphere of oxygen. The laser operated in the TEM_{00} mode with a pulse repetition rate of 1 kHz and a peak power of 23 kW. The laser beam skimmed the diamond surface at an inclination angle of 7° and was focussed to different depths relative to the surface. A peak-to-valley roughness of 3 μm could be obtained by this process. Several authors have used variations of Yoshikawa's method to polish CVD diamond (53,54)

Protrusions that sometimes grow on the diamond surface must be removed prior to polishing. Harker et al. (53) have used reactive plasma etching to remove

such protrusions. In order to etch only the protrusions and not the surrounding material, a nonreactive gold coating was applied to the entire surface. The protrusions were then exposed for reactive plasma etching with oxygen.

CONCLUSION

The combination of superior properties that diamond possesses make this material desirable for many applications. Synthesis of diamond from the gas phase can make it possible to take advantage of these properties because it allows us to deposit diamond over large areas and with thicknesses previously not available. At present, this material is polycrystalline in nature; however, recent results suggest that large area single-crystal diamond may soon be produced. The implications are important for many diverse technical areas: mechanical, electrical, optical, electronic, thermal, etc. The economic impact is expected to grow as new advances are made. The rapid advances being made in diamond processing technology are expected to soon bring many commercial products to the market.

ACKNOWLEDGEMENT

The work was supported in part by the United States Office of Naval Research.

REFERENCES

1. Bundy, F.P., Hall, H.T., Strong, H.M. and Wentorf, R.H., Man-Made Diamonds, Nature 176:51-55 (1955).

2. Anthony, T.R., Banholzer, W.F., Fleischer, J.F., Wei, L., Kuo, P.K., Thomas, R.L. and Pryor, R.W., Thermal Diffusivity of Isotopically Enriched ^{12}C Diamond, Phys. Rev. B 42:1104-1111 (1990).

3. Eversole, W.G., U.S. Patents 3030187 and 3030188 (1962); Kiffer, A.D., Synthesis of Diamond from Carbon Monoxide, Tonowanda Laboratories, Linde Air Products Co., Tonowanda NY, 1956; see footnote 16 in Angus J.C. and Hayman, C., Low Pressure Growth of Diamond and 'Diamondlike' Phases, Science 241:913-921 (1988)

4. Deryagin, B.V. and Fedoseev, D.V., Epitaxial Synthesis of Diamond in the Metastable Region, Russian Chemical Reviews 39:783-788 (1970).

5. Poferi, D.J., Gardner, N.C. and Angus, J.C., Growth of Boron-Doped Diamond Seed Crystals by Vapor Deposition, J. Appl. Phys. 44:1428-1434 (1973).

6. Varnin, V.P., Deryagin, B.V., Fedoseev, D.V., Teremetskaya, I.G. and Khodan, A.N., Growth of Polycrystalline Diamond Films from the Gas Phase, Sov. Phys. Crystallogr. 22:513-515 (1977).

7. Patterson, D.E., Bai, B.J., Chu, C.J., Hauge, R.H. and Margrave, J.L., Halogen-Assisted

Chemical Vapor Deposition of Diamond, in: *New Diamond Science and Technology* (R. Messier, J.T. Glass, J.E. Butler, and R. Roy, eds.), pp. 433-438, Materials Research Society, Pittsburgh, PA (1991).

8. Matsumoto, S., Sato, Y., Kamo, M. and Setaka, N., Vapor Deposition of Diamond Particles from Methane, Jpn. J. Appl. Phys. 21:L183-L185 (1982).

9. Kamo, M., Sato, Y., Matsumoto, S. and Setaka, N., Diamond Synthesis from Gas Phase in Microwave Plasma, J. Cryst. Growth 62:642-644 (1983).

10. Matsumoto, S., Synthesis of Diamond by Plasma CVD and Its Characterization, in: Symp. Proc. International Symposium Plasma Chem., 7th, pp. 79-84 (1985).

11. Hirose, Y. and Kondo, N., Program and Book of Abstracts, Japan Applied Physics 1988 Spring Meeting, March 29, 1988, p.434; Hanssen, L.M., Carrington, W.A., Butler, J.E. and Snail, K.A., Diamond Synthesis Using an Oxygen-Acetylene Torch, Materials Letters 7:289-292 (1991).

12. Narayan, J., Godbole, V.P. and White, C.W., Laser Method for Synthesis and Processing of Continuous Diamond Films on Nondiamond Surfaces, Science 252:416-418 (1991).

13. Spitsyn, B.V., Bouilov, L.L. and Derjaguin, B.V., Vapor Growth of Diamond on Diamond and Other Surfaces, J. Cryst. Growth 52:219-226

(1981); Spitsyn, B.V., The State of the Art in Studies of Diamond Synthesis from the Gaseous Phase and Some Unsolved Problems, in: *Applications of Diamond Films and Related Materials*, (Y. Tzeng, M. Yoshikawa, M. Murakawa and A. Feldman, eds.) pp. 475-482, Elsevier, Amsterdam, 1991)

14. Chiang, C.-P., Flamm, D.L., Ibbotson, D.E. and Mucha, J.A., Diamond Crystal Growth by Plasma Chemical Vapor Deposition, J. Appl. Phys. 63:1744-1748 (1988).

15. Ravi, K.V., Alternating Chemistry Synthesis of Diamond in: Proceedings of the Second International Symposium on Diamond Materials, The Electrochemical Society, Pennington, NJ, in press.

16. Suzuki, K., Yasuda, J. and Inuzuka, T., Growth of Diamond by DC Plasma Chemical Vapor Deposition, Appl. Phys. Lett. 50:728-729 (1987).

17. Matsumoto, S., Hino, M. and Kobayashi, T., Synthesis of Diamond in a RF Induction Thermal Plasma, Appl. Phys. Lett. 51:737-739 (1987).

18. Ohtake, N., Tokura, H., Kuriyama, Y., Mashimo, Y. and Yoshikawa, Y., Sythesis of Diamond Film by Arc Discharge Plasma CVD, in: *Diamond and Diamond-Like Films*, Proceedings Volume 89-12 (J.P. Dismukes, A.J. Purdes, K.E. Spear, B.S. Meyerson, K.V. Ravi, T.D. Moustakas, and M. Yoder, eds.) pp. 93-105, The Electrochem. Society, Pennington, NJ (1989).

19. Angus J.C. and Hayman, C., Low Pressure Growth of Diamond and 'Diamondlike' Phases, Science 241:913-921 (1988)

20. Moravec, T.J. and Orent, T.W., Electron Spectroscopy of Ion Beam and Hydrocarbon Plasma Generated Diamondlike Carbon Films, J. Vac. Sci. Technol. 18:226-228 (1981).

21. Lurie, P.G. and Wilson, J.M., The Diamond Surface II. Secondary Electron Emission, Surface Science 65:476-498 (1977).

22. Wang, Y., Chen, H., Hoffman, R.W. and Angus, J.C., Structural Analysis of Hydrogenated Diamond-like Carbon Films from Electron Energy Loss Spectroscopy, J. Mater. Res. 5:2378-2386 (1990).

23. Solin S.A. and Ramdas, A.K., Raman Spectrum of Diamond, Phys. Rev. B 1:1687-1689 (1970).

24. Robins, L.H., Farabaugh, E.N. and Feldman, A. Line Shape Analysis of the Raman Spectrum of Diamond Films Grown by Hot-filament and Microwave-Plasma Chemical Vapor Deposition, J. Mater. Res. 5:2456-2468 (1990).

25. Badzian. A.R., Badzian, T., Roy, R., Messier, R. and Spear, K.E., Crystallization of Diamond Crystals and Films by Microwave Assisted CVD (Part II) Mat. Res. Bull. 23:531-548 (1988).

26. Ono, A., Baya, T., Funamoto, H. and Nishikawa, A., Thermal Conductivity of Diamond Films Synthesized by Microwave Plasma CVD, Jap. J.

Appl. Phys 25:L808-L810 (1986).

27. Morelli, D.T., Beetz, C.P. and Perry, T.A., Thermal Conductivity of Synthetic Diamond Films, J. Appl. Phys. 64:3063-3066 (1988).

28. Albin, S., Winfree, W. and Scott, B.S., Thermal Diffusivity of Diamond Films in: SPIE Vol. 1146, *Diamond Optics II* (A. Feldman and S. Holly, eds), pp. 85-94, SPIE, Bellingham, WA (1990).

29. Feldman, A., Frederikse, H.P.R. and Norton, S.J., Analysis of Thermal Wave Propagation in Diamond Films, in: SPIE Vol. 1325, *Diamond Optics III* (A. Feldman and S. Holly, eds), pp. 304-314, SPIE, Bellingham, WA (1990).

30. Lu, G. and Swan, W.T., Measurement of Thermal Diffusivity of CVD Diamond by the Converging Thermal Wave Technique, Appl. Phys. Lett. in press.

31. Cielo, P., Utracki, L.A. and Lamontagne, M., Thermal-Diffusivity Measurements by the Converging-Thermal-Wave Technique, Can. J. Phys. 64:1172-1177 (1986).

32. Johnson C.E. and Weimer, W.A., Optical Properties of Microwave-Plasma-Assisted-CVD Diamond Film, in: SPIE Vol. 1146, *Diamond Optics II* (A. Feldman and S. Holly, eds), pp. 188-191, SPIE, Bellingham, WA (1990).

33. Feng, T., Correlation of Optical Properties and Surface Roughness of Polycrystalline Diamond Films, in: SPIE Vol. 1146, *Diamond Optics II* (A. Feldman and S. Holly, eds), pp. 159-165, SPIE,

Bellingham, WA (1990).

34. Snail, K.A., Hanssen, L.M., Morrish, A.A. and Carrington, W.A., Hemispherical Transmittance of Several Free Standing Diamond Films, in: SPIE Vol. 1146, *Diamond Optics II* (A. Feldman and S. Holly, eds), pp. 144-151, SPIE, Bellingham, WA (1990).

35. Cong, Y., Collins, R.W., Epps, G.F. and Windischmann, H., Spectroellipsometry Characterization of Optical Quality Vapor-Deposited Diamond Thin Films, Appl. Phys. Lett. 58:819-821 (1991).

36. Akerman, M.A., McNeely, J.R. and Clausing, R.E., Optical Characterization of Polycrystalline Diamond Films, in: SPIE Vol. 1325, *Diamond Optics III* (A. Feldman and S. Holly, eds), pp. 178-186, SPIE, Bellingham, WA (1990).

37. Wang, X.H., Pilione, L., Zhu, W., Yarbrough, W., Drawl, W. and Messier, R., Infrared Measurements of CVD Diamond Films, in: SPIE Vol. 1325, *Diamond Optics III* (A. Feldman and S. Holly, eds), pp. 160-167, SPIE, Bellingham, WA (1990).

38. Bi, X.X., Eklund, P.C., Zhang, J.G., Rao, A.M., Perry, T.A. and Beetz, C.P. Jr., Optical Properties of Chemical Vapor Deposited Diamond Films, J. Mater. Res. 5:811-817 (1990); Bi, X.X., Eklund, P.C., Zhang, J.G., Rao, A.M., Perry, T.A. and Beetz, C.P. Jr., Optical Tranmission and Reflection of Freestanding Filament Assisted CVD Diamond Films, in: SPIE Vol. 1146, *Diamond Optics II* (A. Feldman and S.

Holly, eds), pp. 192-200, SPIE, Bellingham, WA (1990).

39. Gatesman, A.J., Giles, R.H., Waldman, J., Bourget, L.P. and Post, R., Optical Properties of Polycrystalline Diamond Films in the Far Infrared, in: SPIE Vol. 1325, *Diamond Optics III* (A. Feldman and S. Holly, eds), pp. 170-177, SPIE, Bellingham, WA (1990).

40. Klein, C., Hartnet, T., Miller, R. and Robinson, C., Lattice Vibrational Modes and Defect-Activated IR Absorptions in CVD Diamond, in: Proceedings of the Second International Symposium on Diamond Materials, The Electrochemical Society, Pennington, NJ, in press.

41. Warren, J.L., Yarnell, J.L., Dolling, G. and Cowley, R.A., Lattice Dynamics of Diamond, Phys. Rev. 158:805-808 (1967).

42. Robins, L.R., Farabaugh, E.N. and Feldman, A., Determination of Optical Constants of Thin Chemical-Vapor-Deposited Diamond Windows from 0.5 to 6.5 eV, in: SPIE Vol. 1534, *Diamond Optics IV* (A. Feldman and S. Holly, eds), SPIE, Bellingham, WA, in press.

43. Rösch, von S., Die Optik des Fabulit, die Farbe des Brewsterwinkels und das Farbspielmoment, Opt. Acta 12:253-260 (1965).

44. Peter, F., Uber Brechungsindizes und Absorptionkonstanten des Diamanten zwischen 644 und 226 mμ, Z. Physik 15:358-368 (1923).

45. Edwards, D.F. and Ochoa, E., Infrared Refractive Index of Diamond J. Opt. Soc. Amer. 71:607-608 (1981); D.F. Edwards and H.R. Philipp, in: *Handbook of Optical Constants of Solids* (E.D. Palik, ed.) pp. 665-673, Academic Press, Orlando, FL (1985).

46. Bowden, F.P. and Hanwell, A.E., The Friction of Clean Crystal Surfaces, Proc. R. Soc. Lond. A295:233-243 (1966).

47. Tabor, D., Friction - the Present State of Our Understanding, J. Lubr. Technol. 103:169-179 (1981).

48. Jahanmir, S., Deckman, D.E., Ives, L.K., Feldman, A. and Farabaugh, E., Tribological Characteristics of Synthesized Diamond Films on Silicon Carbide, Wear 133:73-81 (1989).

49. Gardos, M.N. and Ravi, K.V., Tribological Behavior of CVD Diamond Films, in: *Diamond and Diamond-Like Films*, Proceedings Volume 89-12 (J.P. Dismukes, A.J. Purdes, K.E. Spear, B.S. Meyerson, K.V. Ravi, T.D. Moustakas, and M. Yoder, eds.) pp. 475-493, The Electrochem. Society, Pennington, NJ (1989).

50. Cardinale, G.F. and Tustison, R.W., Mechanical Property Measurement of Polycrystalline Diamond Films, in: SPIE Vol. 1325, *Diamond Optics III* (A. Feldman and S. Holly, eds), pp. 90-98, SPIE, Bellingham, WA (1990).

51. McSkimin, H.J., Andreatch, P. Jr. and Glynn, P.,

Elastic Stiffness Moduli of Diamond, J. Appl. Phys. 43:985-987 (1972).

52. Yoshikawa, M., Development and Performance of a Diamond Film Polishing Apparatus with Hot Metals, in: SPIE Vol. 1325, *Diamond Optics III* (A. Feldman and S. Holly, eds), pp. 210-221, SPIE, Bellingham, WA (1990).

53. Harker, A.B., Flintoff, J. and DeNatale, J.F., The polishing of polycrystalline diamond films, in: SPIE Vol. 1325, *Diamond Optics III* (A. Feldman and S. Holly, eds), pp. 222-229, SPIE, Bellingham, WA (1990).

54. Thorpe, T.P., Morrish, A.A., Hanssen, L.M., Butler, J.E. and Snail, K.A., Growth, polishing, and optical scatter of diamond thin films, in: SPIE Vol. 1325, *Diamond Optics III* (A. Feldman and S. Holly, eds), pp. 230-237, SPIE, Bellingham, WA (1990).

FIGURES

Figure 1. Schematic diagram of diamond deposition as described by Spitsyn (13). The gas consists of hydrogen, atomic hydrogen, methane, acetylene, and other hyrocarbons.

Figure 2. Schematic diagram of hot filament CVD reactor for depositing diamond.

Figure 3. Schematic diagram of microwave plasma CVD reactor for depositing diamond.

Figure 4. Linear thermal expansion of diamond and several other materials.

Figure 5. Morphologies of films grown in a hot filament CVD reactor: a) triangular {111} morphology; b) {110} morphology; c) {100} morphology; d) "cauliflower" morphology.

Figure 6. X-ray diffraction patterns of: a) natural diamond powder and b) of CVD diamond produced at NIST.

Figure 7. Raman spectra of a CVD diamond film and a CVD diamond particle.

Figure 8. Cathodoluminescence image of diamond particles and the corresponding SEM image.

Figure 9. Cathodoluminescence spectrum of CVD diamond film showing principal spectral features.

Figure 10. Transmission spectrum of CVD diamond measured by Gatesman et al. (38). (Reprinted with permission of the author.)

FIGURE 11. Transmission spectrum of an optically transparent diamond film.

Figure 12. Friction coefficient as a function of contact load for SiC aginst SiC and SiC against diamond ball-on-flat tests.

6 March 1991

FY91 ONR DOMES ARI CONTRACTORS

Dr. Duncan W. Brown
Advanced Technology Materials, Inc.
520-B Danbury Road
New Milford, CT 06776
(203) 355-2681

Dr. Mark A. Cappelli
Stanford University
Mechanical Engineering Dept.
Stanford, CA 94305
(415) 723-1745

Dr. R. P. H. Chang
Materials Science & Engineering Dept.
2145 Sheridan Road
Evanston, IL 60208
(312) 491-3598

Dr. Bruce Dunn
UCLA
Chemistry Department
Los Angeles, CA 90024
(213) 825-1519

Dr. Al Feldman
Leader, Optical Materials Group
Ceramics Division
Materials Science & Engineering Lab
NIST
Gaithersburg, MD 20899
(301) 975-5740

Dr. John Field
Department of Physics
University of Cambridge
Cavendish Laboratory
Madingley Road
Cambridge CB3 OHE
England
44-223-337733, ext. 7318

Dr. William A. Goddard, III
Director, Materials and Molecular
Simulation Center
Beckman Institute
California Institute of Technology
Pasadena, CA 91125
(818) 356-6544
Fax: (818) 568-8824

Dr. David Goodwin
California Institute of Technology
Mechanical Engineering Dept.
Pasadena, CA 91125
(818) 356-4249

Dr. Alan Harker
Rockwell Int'l Science Center
1049 Camino Dos Rios
P.O. Box 1085
Thousand Oaks, CA 91360
(805) 373-4131

Mr. Stephen J. Harris
General Motors Research Laboratories
Physical Chemistry Department
30500 Mound Road
Warren, MI 48090-9055
(313) 986-1305
Fax: (313) 986-8697
E-mail: sharris@gmr.com

Dr. Rudolph A. Heinecke
Standard Telecommunication
Laboratories, Ltd.
London Road
Harlow, Essex CM17 9MA
England
44-279-29531, ext. 2284

Dr. Kelvin Higa
Code 3854
Naval Weapons Center
China Lake, CA 93555-6001

Dr. Curt E. Johnson
Code 3854
Naval Weapons Center
China Lake, CA 93555-6001
(619) 939-1631

Dr. J. J. Mecholsky, Jr.
University of Florida
Materials Science & Engineering Dept.
256 Rhines Hall
Gainesville, FL 32611
(904) 392-1454

Dr. Rishi Raj
Cornell University
Materials Science & Engineering Dept.
Ithaca, NY 14853
(607) 255-4040

Dr. Rustum Roy
Pennsylvania State University
Materials Research Laboratory
University Park, PA 16802
(814) 865-2262

Dr. James A. Savage
Royal Signals & Radar Establishment
St. Andrews Road
Great Malvern, Worcs WR14.3PS
England
01-44-684-895043

Dr. Y. T. Tzeng
Auburn University
Electrical Engineering Dept.
Auburn, AL 36849
(205) 884-1869

Dr. Terrell A. Vanderah
Code 3854
Naval Weapons Center
China Lake, CA 93555-6001
(619) 939-1654

Dr. George Walrafen
Howard University
Chemistry Department
525 College Street N.W.
Washington, D.C. 20059
(202) 636-6897/6564

Dr. Aaron Wold
Brown University
Chemistry Department
Providence, RI 02912
(401) 863-2857

Dr. Wally Yarborough
Pennsylvania State University
Materials Research Laboratory
University Park, PA 16802
(814) 865-7102

6 March 1991

DISTRIBUTION LIST

Mr. James Arendt
Hughes Aircraft Company
8433 Fallbrook Ave. 270/072
Canoga Park, CA 91304
(838) 702-2890

Mr. Larry Blow
General Dynamics
1525 Wilson Blvd., Suite 1200
Arlington, VA 22209
(703) 284-9107

Mr. Ellis Boudreaux
Code AGA
Air Force Armament Laboratory
Eglin AFB, FL 32542

Dr. Duncan W. Brown
Advanced Technology Materials, Inc.
520-B Danbury Road
New Milford, CT 06776
(203) 355-2681

Dr. Mark A. Cappelli
Stanford University
Mechanical Engineering Dept.
Standford, CA 94305
(415) 723-1745

Dr. R. P. H. Chang
Materials Science & Engineering Dept.
2145 Sheridan Road
Evanston, IL 60208
(312) 491-3598

Defense Documentation Center
Cameron Station
Alexandria, VA 22314
(12 copies)

Dr. Al Feldman
Leader, Optical Materials Group
Ceramics Division
Materials Science & Engineering Lab
NIST
Gaithersburg, MD 20899
(301) 975-5740

Dr. John Field
Department of Physics
University of Cambridge
Cavendish Laboratory
Madingley Road
Cambridge CB3 OHE
England
44-223-337733, ext. 7318

Dr. William A. Goddard, III
Director, Materials and Molecular
Simulation Center
Beckman Institute
California Institute of Technology
Pasadena, CA 91125
(818) 356-6544
Fax: (818) 568-8824

Dr. David Goodwin
California Institute of Technology
Mechanical Engineering Dept.
Pasadena, CA 91125
(818) 356-4249

Dr. Kevin Gray
Norton Company
Goddard Road
Northboro, MA 01532
(508) 393-5968

Mr. Gordon Griffith
WRDC/MLPL
Wright-Patterson AFB, OH 45433

Dr. H. Guard
Office of Chief of Naval Research
(ONR Code 1113PO)
800 North Quincy Street
Arlington, VA 22217-5000

Dr. Alan Harker
Rockwell Int'l Science Center
1049 Camino Dos Rios
P.O. Box 1085
Thousand Oaks, CA 91360
(805) 373-4131

Mr. Stephen J. Harris
General Motors Research Laboratories
Physical Chemistry Department
30500 Mound Road
Warren, MI 48090-9055
(313) 986-1305
Fax: (313) 986-8697
E-mail: sharris@gmr.com

Dr. Rudolph A. Heinecke
Standard Telecommunication
Laboratories, Ltd.
London Road
Harlow, Essex CM17 9MA
England
44-279-29531, ext. 2284

Dr. Curt E. Johnson
Code 3854
Naval Weapons Center
China Lake, CA 93555-6001
(619) 939-1631

Dr. Larry Kabacoff (Code R32)
Officer in Charge
Naval Surface Weapons Center
White Oak Laboratory
10901 New Hampshire
Silver Spring, MD 20903-5000

Mr. M. Kinna
Office of Chief of Naval Research
(ONT Code 225)
800 North Quincy Street
Arlington, VA 22217-5000

Dr. Paul Klocek
Texas Instruments
Manager, Advanced Optical Materials Branch
13531 North Central Expressway
P.O. Box 655012, MS 72
Dallas, Texas 75268
(214) 995-6865

Ms. Carol R. Lewis
Jet Propulsion Laboratory
4800 Oak Grove Drive
Mail Stop 303-308
Pasadena, CA 91109
(818) 354-3767

Dr. J. J. Mecholsky, Jr.
University of Florida
Materials Science & Engineering Dept.
256 Rhines Hall
Gainesville, FL 32611
(904) 392-1454

Dr. Russ Messier
Pennsylvania State University
Materials Research Laboratory
University Park, PA 16802
(814) 865-2262

Mr. Mark Moran
Code 3817
Naval Weapons Center
China Lake, CA 93555-6001

Mr. Ignacio Perez
Code 6063
Naval Air Development Center
Warminster, PA 18974
(215) 441-1681

Mr. C. Dale Perry
U.S. Army Missile Command
AMSMI-RD-ST-CM
Redstone Arsenal, AL 35898-5247

Mr. Bill Phillips
Crystallume
125 Constitution Drive
Menlo Park, CA 94025
(415) 324-9681

Dr. Rishi Raj
Cornell University
Materials Science & Engineering Dept.
Ithaca, NY 14853
(607) 255-4040

Dr. M. Ross
Office of Chief of Naval Research
(ONR Code 1113)
800 North Quincy Street
Arlington, VA 22217-5000

Dr. Rustum Roy
Pennsylvania State University
Materials Research Laboratory
University Park, PA 16802
(814) 865-2262

Dr. James A. Savage
Royal Signals & Radar Establishment
St. Andrews Road
Great Malvern, Worcs WR14.3PS
England
01-44-684-895043

Mr. David Siegel
Office of Chief of Naval Research
(ONT Code 213)
800 North Quincy Street
Arlington, VA 22217-5000

Dr. Keith Snail
Code 6520
Naval Research Laboratory
Washington, D.C. 20375
(202) 767-0390

Dr. Y. T. Tzeng
Auburn University
Electrical Engineering Dept.
Auburn, AL 36849
(205) 884-1869

Dr. George Walrafen
Howard University
Chemistry Department
525 College Street N.W.
Washington, D.C. 20054
(202) 806-6897/6564

Mr. Roger W. Whatmore
Plessey Research Caswell Ltd.
Towcester Northampton NN128EQ
England
(0327) 54760

Dr. Charles Willingham
Raytheon Company
Research Division
131 Spring Street
Lexington, MA 02173
(617) 860-3061

Dr. Robert E. Witkowski
Westinghouse Electric Corporation
1310 Beulah Road
Pittsburgh, PA 15235
(412) 256-1173

Dr. Aaron Wold
Brown University
Chemistry Department
Providence, RI 02912
(401) 863-2857

Mr. M. Yoder
Office of Chief of Naval Research
(ONR Code 1114SS)
800 North Quincy Street
Arlington, VA 22217-5000